

Microscale imaging sheds light on species-specific strategies for photo-regulation and photo-acclimation of microphytobenthic diatoms

Bruno Jesus¹  | Thierry Jauffrais^{2,3}  | Erik Trampe⁴ | Vona Méléder¹ |
Lourenço Ribeiro⁵ | Joan M. Bernhard⁶ | Emmanuelle Geslin³ | Michael Kühl⁴ 

¹Nantes Université, Institut des Substances et Organismes de la Mer, ISOMer, UR2160, Nantes, France

²Ifremer, IRD, Univ Nouvelle-Calédonie, Univ La Réunion, CNRS, UMR 9220 ENTROPIE, RBE/LEAD, Noumea, New Caledonia

³Université d'Angers, Nantes Université, Le Mans Université, Angers, France

⁴Marine Biological Section, Department of Biology, University of Copenhagen, Helsingør, Denmark

⁵MARE – Marine and Environmental Sciences Centre/ARNET – Aquatic Research Network Associated Laboratory, Faculty of Sciences, University of Lisbon, Lisbon, Portugal

⁶Geology and Geophysics Department, Woods Hole Oceanographic Institution, Woods Hole, Massachusetts, USA

Correspondence

Bruno Jesus, Nantes Université, Institut des Substances et Organismes de la Mer, ISOMer, UR2160, Nantes F-44000, France.
Email: bruno.jesus@univ-nantes.fr

Michael Kühl, Marine Biological Section, Department of Biology, University of Copenhagen, Strandpromenaden 5, DK 3000 Helsingør, Denmark.
Email: mkuhl@bio.ku.dk

Funding information

European Union's Horizon 2020 research and innovation programme, Grant/Award Number: Marie Skłodowska-Curie grant agreement N° 860125; Independent Research Fund Denmark, Grant/Award Number: DFF-8022-00301B; Region Pays de Loire, Grant/Award Number: University of Angers (France); WHOI's Investment in Science Program

Abstract

Intertidal microphytobenthic (MPB) biofilms are key sites for coastal primary production, predominantly by pennate diatoms exhibiting photo-regulation via non-photochemical quenching (NPQ) and vertical migration. Movement is the main photo-regulation mechanism of motile (epipellic) diatoms and because they can move from light, they show low-light acclimation features such as low NPQ levels, as compared to non-motile (epipsammic) forms. However, most comparisons of MPB species-specific photo-regulation have used low light acclimated monocultures, not mimicking environmental conditions. Here we used variable chlorophyll fluorescence imaging, fluorescent labelling in sediment cores and scanning electron microscopy to compare the movement and NPQ responses to light of four epipellic diatom species from a natural MPB biofilm. The diatoms exhibited different species-specific photo-regulation features and a large NPQ range, exceeding that reported for epipsammic diatoms. This could allow epipellic species to coexist in compacted light niches of MPB communities. We show that diatom cell orientation within MPB can be modulated by light, where diatoms oriented themselves more perpendicular to the sediment surface under high light vs. more parallel under low light, demonstrating behavioural, photo-regulatory response by varying their light absorption cross-section. This highlights the importance of considering species-specific responses and understanding cell orientation and photo-behaviour in MPB research.

This is an open access article under the terms of the [Creative Commons Attribution](https://creativecommons.org/licenses/by/4.0/) License, which permits use, distribution and reproduction in any medium, provided the original work is properly cited.

© 2023 The Authors. *Environmental Microbiology* published by Applied Microbiology International and John Wiley & Sons Ltd.

INTRODUCTION

Estuarine intertidal ecosystems are highly productive and biodiverse environments (Pinckney, 2018), where primary production is strongly driven by assemblages of benthic microalgae and photosynthetic bacteria, collectively known by the name microphytobenthos (MPB) (MacIntyre et al., 1996). When these microorganisms are motile they form transient biofilms by accumulating at the sediment surface during diurnal low-tide periods (Serôdio et al., 1997) and carry out keystone ecosystem functions (Hope et al., 2019). They are important food sources for primary consumers (Middelburg et al., 2000), they mediate nutrient fluxes at the sediment interface (Cabrita & Brotas, 2000; Dong et al., 2000), they stabilize the sediments (Paterson, 1989) and they can contribute up to 50% of estuarine primary productivity (Underwood & Kromkamp, 1999). While MPB can be taxonomically diverse, pennate diatoms are predominant in temperate and Arctic systems (Glud et al., 2009; Jesus et al., 2009; MacIntyre et al., 1996; McIntire & Moore, 1977; Ribeiro et al., 2021; Serôdio & Paterson, 2020).

Sediment type has an important role in structuring diatom community structure in MPB, both in terms of overall diversity and in the growth forms that dominate the microbial assemblages (Jesus et al., 2009; Ribeiro et al., 2013; Ribeiro et al., 2021; Underwood et al., 2022; Weilhoefer et al., 2021). The two main diatom growth forms in intertidal sediments are epipellic, that is, living freely and in between sediment particles, and epipsammic, that is, living attached or in very close association with sediment particles (Round, 1971; Sabbe, 1997). Epipellic diatoms predominate in silty sediments (mud), while epipsammic diatoms predominate in sandy sediments (Méléder et al., 2007; Ribeiro et al., 2021; Rivera-Garcia et al., 2017; Weilhoefer et al., 2021).

Intertidal benthic diatoms live in a highly dynamic, stressful environment (Admiraal, 1984) but exhibit high primary productivity rates (Frankenbach et al., 2020) and show few signs of photo-inhibition under natural conditions (Cartaxana et al., 2011; Kromkamp et al., 1998; Perkins et al., 2010); this is generally attributed to highly efficient energy dissipation photo-regulation mechanisms in benthic diatoms achieved by combining movement with the capacity of reaching unusually high non-photochemical quenching (NPQ) values (Lavaud et al., 2002; Ruban et al., 2004; Wilhelm et al., 2014). Exposure to high light can result in oxidative damage to photosystem II (PSII) in diatoms (Cartaxana et al., 2013), but benthic diatoms can employ short-term photo-regulation mechanisms such as non-photochemical quenching (NPQ) associated with the xanthophyll cycle and vertical migration

movements to optimize light requirements for photosynthesis under fluctuating light (Cartaxana et al., 2011; Laviale et al., 2015; Perkins et al., 2010). The NPQ associated with the xanthophyll cycle (NPQ-xc) is a well-known physiological light-dependent process, where the xanthophyll diadinoxanthin is de-epoxidised and converted to diatoxanthin; the latter dissipates excess light as heat (Blommaert et al., 2021). Comparing NPQ light response curves, i.e., measurements of NPQ as a function of photon irradiance, is a common method to infer the capacity of diatoms in coping with excess light (Serôdio & Lavaud, 2011). Diatom species with higher NPQ capacity typically show a sigmoidal response to increasing light levels, composed of an initial lag period with no NPQ followed by an increase in NPQ until it reaches a stable maximum level. Diatoms acclimated to lower light levels or with lower NPQ capacity often lack the initial lag period and exhibit a rapid increase in NPQ that levels off at lower overall NPQ levels (Serôdio & Lavaud, 2011).

It is commonly assumed that movement is the main photo-regulation mechanism of epipellic diatoms, while epipsammic, non-motile species predominantly use NPQ-xc as their main photo-regulation mechanism (Barnett et al., 2015; Cartaxana et al., 2011; Jesus et al., 2009). It has also been shown that some correlation exists between diatom-growth form and how their NPQ is regulated by light (Barnett et al., 2015; Blommaert et al., 2017; Blommaert et al., 2018; Derks & Bruce, 2018; Méléder et al., 2018). It is hypothesised that there is a gradual change from high NPQ capacity in epipsammic non-motile diatoms towards low NPQ capacity in epipellic motile diatoms, based on the rationale that non-motile epipsammic diatoms—which are attached to sediment grains—need to rely more in photo-physiological regulation, while epipellic motile diatoms can move away from light and thus can harbour larger light harvesting antennas (Barnett et al., 2015; Jesus et al., 2009). However, most studies comparing the species-specific photo-regulation capacity of epipellic versus epipsammic diatoms have used diatom cultures acclimated to very low light levels (from 20 to 75 $\mu\text{mol photons m}^{-2} \text{s}^{-1}$; 400–700 nm) (Barnett et al., 2015; Blommaert et al., 2017; Blommaert et al., 2018; Derks & Bruce, 2018) in comparison to in-situ photon irradiance (Jesus et al., 2009; Serôdio & Catarino, 1999). Hence, such comparative studies might not be representative of MPB photo-regulation patterns under natural conditions—which are likely to be more complex.

Epipellic biofilms are often composed of dozens of different species strongly concentrated in the top 1 mm of the sediment (Cartaxana et al., 2011; Jesus et al., 2009; Yallop et al., 1994). Light attenuation in fine-grained muddy sediments is very high (Cartaxana et al., 2016; Kühl & Jørgensen, 1994), often restricting

the photic zone to 500 μm (Cartaxana et al., 2011; Cartaxana et al., 2016). This creates an environment where light is a limited resource distributed in a steep vertical gradient and this most likely increases the selective pressure for species with different light requirements and strategies for optimal light harvesting modulating cell structure, behaviour and photo-physiology. Most studies on natural MPB biofilm photo-physiology have been done on intact biofilms (Brotas et al., 2003; Cartaxana et al., 2011; Cartaxana et al., 2016; Cruz & Serôdio, 2008; Jesus et al., 2009; Kromkamp et al., 1998; Lefebvre et al., 2011; Perkins et al., 2001; Perkins et al., 2010; Prins et al., 2020; Serôdio, Cruz, et al., 2005; Serôdio, Vieira, et al., 2005), providing an integrated biofilm response that combines all species-specific responses. With the exception of Underwood et al. (2005) no studies exist on the characterization of natural (i.e., from freshly collected sediments) MPB species-specific photo-regulation mechanisms.

Our study addresses this knowledge gap by comparing the photo-physiological responses of different epipelagic diatom species from a natural biofilm to experimental changes in light exposure. We used microscopic variable chlorophyll fluorescence imaging to characterize species-specific changes in photosynthetic capacity curves in combination with studies of diatom cell organization and migration in structured biofilms using fluorescently labelled embedded cores (FLEC) together with low-temperature scanning electron microscopy.

EXPERIMENTAL PROCEDURES

Study site and general experimental setup

Sediment with visible microphytobenthic biofilms was collected by scraping the sediment surface (1–2 mm) of Bourgneuf Bay mudflats (47.013° N, 2.019° W) in April 2017. The sediment was brought back to the laboratory, homogenized by mixing and left overnight to settle in trays with water from the site at in situ temperature (17°C) and salinity (33 ppt). Diatom biofilms were naturally restructured the next day in synchronization with low tide, following their endogenous rhythm (Serôdio et al., 1997). The overlaying water was then gently removed and the biofilm was left to migrate upward at low photon irradiance (LL, 70 $\mu\text{mol photons m}^{-2} \text{s}^{-1}$; 400–700 nm) under a LED panel light source (FytoScope FS 130-WIR).

Thirty minutes before the in situ time of low tide, we exposed half of the sediment to 1 h of high photon irradiance (HL, 1000 $\mu\text{mol photons m}^{-2} \text{s}^{-1}$; 400–700 nm) also with a LED panel light source (FytoScope FS 130-WIR), while the other half was kept at LL.

Extracting diatom cells from the sediment

Diatom cells for single-cell variable chlorophyll fluorescence imaging (see below) were extracted from the sediment using the lens tissue method (Eaton & Moss, 1966). Lens tissues (20 by 20 cm) were placed on top of the sediment immediately after removing the overlaying water and left for 3 h before being removed. Cells were then gently removed from the lens tissues using filtered seawater from the site. All lens tissues were pooled and the cell suspension was left at very low photon irradiance (5 $\mu\text{mol photons m}^{-2} \text{s}^{-1}$; 400–700 nm) before onset of the variable fluorescence measurements. An extra set of lens tissues (2 by 2 cm, $n = 3$, total surface 12 cm^2) were left in place and removed after only 1 h of light treatment, HL and LL, respectively. These additional samples were pooled by treatment and stored in a 2.5% glutaraldehyde solution and kept for diatom species analysis, which was done using frustule structures as species determinant. Observation and identification was done on cells cleaned by cremation (450°C for 2 h) and embed in Naphrax (Brunel Microscopes Ltd., Chippenham, Wiltshire, United Kingdom). Diatom cell counts were done twice on material from the lens tissue samples, once counting all species within ~ 400 valves or 100 fields at 40 \times magnification and a second time counting the entire slide but including only the larger species (i.e., those subject to photo-physiological measurements: *Gyrosigma limosum*, *Plagiotropis vanheurckii*, *Plagiotropis neovitrea*, *Pleurosigma angulatum*, *Pleurosigma aestuarii*). When including the smaller species in the counting, the threshold of 400 valves or 100 fields was reached very quickly and the bigger species might have been underrepresented. Focusing only on the bigger species allowed enumeration of the entire slide; significantly increasing the counts of the bigger species (6.5 \times more) and increasing our confidence in the observed differences between light conditions.

Variable chlorophyll fluorescence imaging

Variable chlorophyll fluorescence measurements were done with the saturation-pulse method (Schreiber et al., 1986) using a microscopic pulse-amplitude modulated (PAM) imaging system (Microscopy Imaging PAM; WALZ, Germany) that was mounted on an epifluorescence microscope (AxioStar plus FL, Zeiss), equipped with a 20 \times -magnification objective (Plan-Apochromate, Zeiss GmbH) and using blue LEDs (450 nm) for measuring light pulses, saturating light pulses and actinic light (Vieira et al., 2013). Samples were mounted on a microscope slide covered by a coverslip and in filtered seawater (2 μm Whatman membrane filters) from the sampling site. To avoid image

blur, all variable chlorophyll fluorescence measurements were done after adding the diatom movement inhibitor Latrunculin A (LatA, 5 μM) to the cell suspensions. This inhibitor is known to have a negligible effect on diatom photosynthesis (Cartaxana & Serôdio, 2008). We studied the photosynthetic capacity of the diatoms in two ways.

Rapid light curves and NPQ: We first measured rapid changes in the effective PSII quantum yield as a function of photon irradiance, that is, so-called rapid light curves (RLC) (Ralph & Gademann, 2005). Each RLC was measured using 12 incremental light steps (0, 22, 34, 43, 46, 53, 88, 129, 162, 213, 375 and 410 $\mu\text{mol photons m}^{-2} \text{s}^{-1}$; 450 nm), each lasting 20 s. Before the start of these measurements, the diatom samples were acclimated to low light for 30 min using very low photon irradiance (5 $\mu\text{mol photons m}^{-2} \text{s}^{-1}$; 400–700 nm) to dissipate any potential NPQ accumulated in the dark. Removing this NPQ component allows true F_o and F_m to be measured, which often is not possible in natural MPB diatoms exposed to complete darkness (Cruz & Serôdio, 2008; Jesus et al., 2006). Consequently, the first measuring point of the RLCs at zero actinic light yielded the minimum fluorescence yield (F_o), and the maximum fluorescence yield (F_m), which were used to calculate the maximum PSII quantum efficiency (F_v/F_m) as $F_v/F_m = (F_m - F_o)/F_m$. Subsequent measurements yielded the fluorescence yield (F) and the maximum fluorescence yield (F_m') in the light-exposed state, which could be used to calculate the effective PSII quantum yield at each experimental light level (E) as $Y_{II} = (F_m' - F)/F_m'$. Subsequently, we calculated the relative PSII electron transport rate at each photon irradiance level as $rETR(E) = Y_{II}(E) \times E$ and the non-photochemical quenching at each photon irradiance level as $NPQ = (F_m - F_m')/F_m'$.

The following parameters were estimated by fitting the RLCs, that is, rETR vs. E curves, with the photosynthesis-light response model of Eilers and Peeters (1988): α , initial RLC slope under light limitation; $rETR_{\text{max}}$, maximum relative electron transport rate; E_k , photon irradiance at onset of light saturation coefficient; and E_{opt} , the photon irradiance where rETR reached its maximal value. When rETR RLC did not show any saturation then the rETR value measured at the highest light level was used as a proxy for $rETR_{\text{max}}$. Such combined RLC and NPQ measurements were carried out on four diatom species that were large enough to have sufficient pixels in the imaging analysis: *Pleurosigma angulatum* (Figure 1A), *Plagiotropis neovitreata* (Figure 1B), *Pleurosigma aestuarii* (Figure 1C) and *Gyrosigma limosum* (Figure 1D).

Light stress induction-recovery: The second set of variable fluorescence measurements consisted of light stress induction-recovery sequences, which consisted of initial dark acclimation and determination of F_v/F_m followed by measurements of F and F_m' at an interval

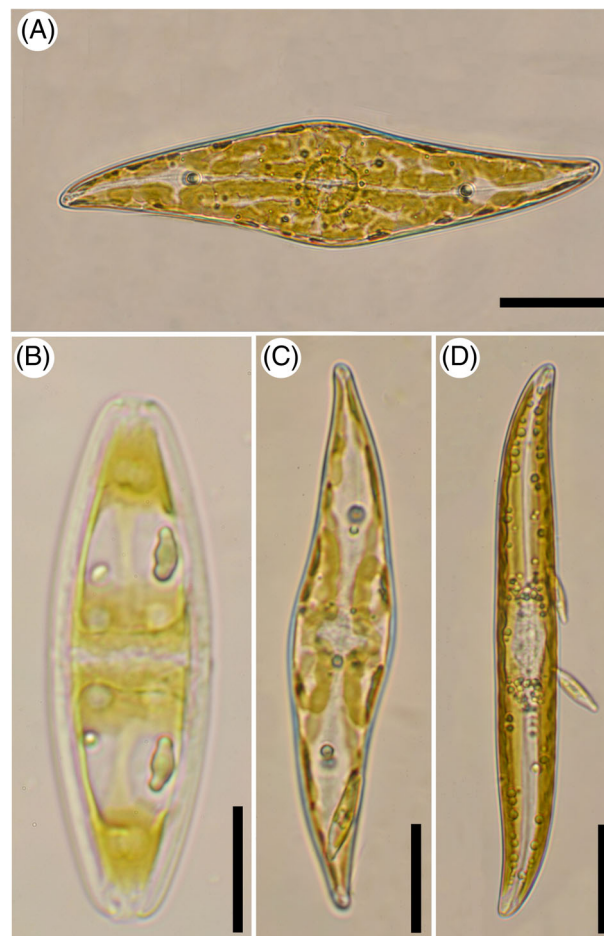


FIGURE 1 Light micrograph of: (A) *Pleurosigma angulatum*. (B) *Plagiotropis neovitreata*. (C) *Pleurosigma aestuarii*. (D) *Gyrosigma limosum*. Scale bars: A = 50 μm , B, C = 25 μm and D = 30 μm .

of 20 s over 4 min of blue light exposure at 400 $\mu\text{mol photons m}^{-2} \text{s}^{-1}$ (450 nm) followed by 15 min of recovery in darkness. This allowed us to measure NPQ induction and recovery at time scales longer than the 20 s used in each of the RLC light steps. The measured fluorescence parameters were: Y_{II} ; $Y(\text{NO}) = F/F_m$, the fraction of light energy that is dissipated via non-regulated mechanisms (Klughammer & Schreiber, 2008); and $Y(\text{NPQ}) = (F/F_m') + (F/F_m)$, the fraction of light energy that is dissipated by photo-protective mechanisms (Klughammer & Schreiber, 2008). Induction-recovery measurements were done only on *Gyrosigma limosum* and *Pleurosigma aestuarii* due to time constraints and in order to ensure enough replication. See Table S1 for list of fluorescence parameters.

Fluorescently labelled embedded core method (FLEC)

The FLEC method is a live-labelling method that allows the visualization of microorganisms in sediments by

combining fluorescent labelling and subsequent fixation of enzymatically active microorganisms with fluid-displacing low viscosity epoxy resin infiltration of undisturbed sediments (Bernhard et al., 2003; Bernhard & Bowser, 1996). In the present case, it was done using three successive steps. (1) Live-labelling: PVC corers (cut-off 10-mL syringes) of 1.1 cm diameter were inserted into the first 2–3 cm of the sediment and incubated overnight in a solution of seawater from the sampling site containing a fluorogenic probe for esterase activity (12 h, 1 μ M CellTracker Green CMFDA, 5-chloromethylfluorescein diacetate; hereafter 'CTG', Molecular Probes, Invitrogen Detection Technologies). The CTG probe slowly perfused each sediment core, permeating all living organisms in the sediment; once in the cell it is cleaved by cellular esterase activity producing a membrane-impermeant fluorescent product in the cells (Bernhard et al., 2003; Bernhard & Bowser, 1996). This labelling method is not disruptive to cellular functions, as it was originally designed to track cells throughout mammalian developmental stages. (2) Fixation: The next day and after submitting the sediment to the two light treatments (i.e., LL and HL), the cores and entrained living-microorganisms were fixed via perfusion—to preserve the microorganisms in their living position—using a solution of 3% glutaraldehyde in 0.1 M cacodylate buffer (pH 7.2). (3) Embedding and imaging: the cores were submitted to a series of desalination and dehydration steps consisting of: three rinses in 0.1 M cacodylate buffer (24 h each) followed by a graded series of ethanol (30%, 50%, 70%, 80%, 90%, 95%, 100%, 100%, 100%, \sim 1 week for each step) and acetone (100% \times 2). The cores were then infiltrated with ultra-low viscosity resin (Spurr, Sigma–Aldrich; Spurr, 1969) using a graded series of resin / acetone mixtures (50%, 70%, 80%, 90%, 100%, 100%, \sim 3 days for each step) and were then finally polymerized at 70°C. The polymerized cores were sectioned vertically with a low speed diamond wheel saw (Minitom, Struers, Denmark) and wet-polished using silicon carbide (30, 15 and 8 μ m) and diamond (1 μ m) powders of decreasing particle size. Once polished, the vertical sections were observed using a confocal laser scanning microscope (405 nm, TCS SP8, LEICA) and a scanning electron microscopy (20 kV, 10.5 mm WD, eSEM, EVO LS10, Zeiss).

Low temperature scanning electron (LTSEM)

Small metallic corers (1 \times 3 cm) were inserted into the first cm of the restructured sediment, collected and immediately cryo-fixed in liquid nitrogen. The frozen sediment surface cores (cryo-cores) were carefully extruded from the coring device and were wrapped in

aluminium foil and placed at -80°C until further treatment. Before analysis, the cryo-cores were placed in liquid nitrogen and quickly cut with a sharp razor blade on a frozen surface to obtain smaller subsamples that fit into the cryo-prep chamber (Quorum PP2000, Quorum Technologies, Laughton, UK) attached to a low temperature scanning electron microscope (EVO LS10 eSEM; ZEISS). After coating, the small cryo-cores were transferred to the SEM to observe the surface of the biofilm and identify diatom species using an accelerating voltage of 7 kV with a working distance of 10.5 mm.

Quantification of cell orientation and depth distribution

Diatom depth distribution was determined from FLEC images using image analysis (*ImageJ*; Schneider et al., 2012) by quantifying pixels with the presence of labelled diatoms, which—due to combination of the red chlorophyll *a* autofluorescence with the GTC—appear in the FLEC images as bright yellow pixels (Figure S1A). First the sediment surface was marked and the sediment background was removed by thresholding the image to a section of the image that was diatom-free (Figure S1B). The image was then converted to a grey 8-bit image and divided in 100- μ m width and 2000- μ m deep transects (Figure S1C). Average pixel values per depth were extracted using the *ImageJ Plot Profile tool*. Distances were manually corrected in relation to the position of the sediment surface for each transect, with the surface being zero, positive values being above, and negative values being below the surface, respectively. All transects were averaged per light condition and standard errors were calculated ($n = 72$ for each condition).

Diatom cell orientation in the biofilm was quantified by drawing a line aligned with the longitudinal axis of each diatom valve and using the *ImageJ* measure tool to quantify the angles of the lines (Figure S2). When diatoms were perpendicular to the point of view they appear as a circle in the image and were drawn as such, which gave them an orientation of zero degrees, that is, parallel to the surface. The number of cells measured in LL was 644 and 670 for HL.

Statistical analysis

Kruskal–Wallis rank sum tests were used to test for differences between the RLC parameters (5% significance level). Repeated measures analyses in the light-stress induction followed by recovery were done with Friedman tests. Post-hoc comparisons were done with pairwise *U*-tests using Wilcoxon rank sum tests.

All statistical analyses were done with the software R (R Core Team, 2020).

RESULTS

Benthic diatom responses to light treatments

Species diversity at the sediment surface

The main diatom species extracted with the lens tissue technique were similar in the two light treatments (Table 1). The most obvious effect of the high light (HL) treatment was the relative increase of *Plagiotropis neovitre*a, *Navicula phyllepta*, *Navicula cf. pargemina* and the disappearance of *Gyrosigma limosum* (Table 1). Counting just the larger species highlighted the differences caused by the light treatment, with *Pleurosigma aestuarii* and *Plagiotropis neovitre*a increasing their relative frequency in HL and the other two species decreasing (Table 1). The analysis of low temperature scanning electron microscopy images also showed few differences in species composition; the major difference under HL was the decrease of *Pleurosigma angulatum* in comparison with *Pleurosigma aestuarii*, and the appearance of *Plagiotropis neovitre*a at the sediment surface (Figure 2A–D). Absolute counts of the large diatoms were also much higher in the LL condition where we counted 8847 specimens in comparison with the HL condition where we counted 1024 specimens for the same sampling surface.

TABLE 1 Diatom assemblage at the two light treatments (relative percentage).

All species	LL (% , n = 1806)	HL (% , n = 258)
<i>Pleurosigma aestuarii</i>	65	48
<i>Navicula cf. wiesneri</i>	14	13
<i>Plagiotropis vanheurckii</i>	5	5
<i>Navicula phyllepta</i>	5	14
<i>Navicula cf. pargemina</i>	5	12
<i>Gyrosigma limosum</i>	2	0
<i>Plagiotropis neovitre</i> a	2	6
<i>Pleurosigma angulatum</i>	1	2
<i>Cymatosira belgica</i>	1	0
Large species	LL (% , n = 8847)	HL (% , n = 1024)
<i>Pleurosigma aestuarii</i>	57	69
<i>Pleurosigma angulatum</i>	1	1
<i>Plagiotropis vanheurckii</i>	35	25
<i>Plagiotropis neovitre</i> a	2	4
<i>Gyrosigma limosum</i>	5	1

Vertical distribution of the biofilm

The two light treatments resulted in different vertical distributions of the diatoms in the sediment biofilm (Figure 3). Under HL, most diatoms migrated deeper into the sediment leaving only a thin diatom layer at the sediment surface (Figure 3A,B; Figure 4A,C,E,G). Under LL incubation, we found a strong accumulation of diatoms forming a multilayered biofilm at the sediment surface (Figure 3C,D)—often with more than 5 distinct diatom layers (Figure 4B,D,F,H). Analysis of the vertical transects showed that LL biofilms peaked at about 60 μm outside the sediment forming a $\sim 100 \mu\text{m}$ thick biofilm, while HL biofilms had their maximum at $-5 \mu\text{m}$ and were dispersed more homogeneously towards deeper sediment layers (Figure 5).

Cell orientation was also significantly different between the two light treatments (Kolmogorov–Smirnov test, p -value = 0.0259), with more HL cells oriented between 40° and 120° than LL cells; here 90° corresponds to cells perpendicular to the sediment surface. LL biofilms showed more cells oriented between 0° and 40° , that is, a cell orientation closer to being parallel to the sediment surface (Figure 6).

Single-cell variable chlorophyll fluorescence

The measurements of relative electron transport rate (rETR) and non-photochemical quenching (NPQ) as a function of photon irradiance exhibited clear species-specific patterns (Figure 7). While *Plagiotropis neovitre*a showed no signs of rETR saturation (Figure 7A) and very low levels of NPQ (Figure 7B), *Pleurosigma aestuarii* exhibited the lowest rETR (Figure 7B) and the highest NPQ levels (Figure 7B). The other two species (*Pleurosigma angulatum*, *Gyrosigma limosum*) showed an intermediate response (Figure 7).

RLC parameters (Figure 8) showed significant differences between species (Kruskal–Wallis, $p < 0.05$). α showed no differences between *G. limosum* and *P. angulatum* ($p < 0.05$) and was higher than in all the other species, while *Plagiotropis neovitre*a and *Pleurosigma aestuarii* α values were lower than the other species and showed no differences between them ($p > 0.05$; Figure 8A). The E_k values differed among all species, with the exception of *P. angulatum* and *P. aestuarii* that were similar ($p > 0.05$; Figure 8B). *Pleurosigma angulatum* showed the lowest E_k values and *Plagiotropis neovitre*a showed the highest ($p < 0.05$; Figure 8B). E_{opt} showed no differences between the two *Pleurosigma* species and also no differences between *G. limosum* and *P. angulatum* ($p > 0.05$; Figure 8C). Overall, E_{opt} values were higher for *Plagiotropis neovitre*a than for all the other species ($p < 0.05$; Figure 8C). rETR_{max} values were different

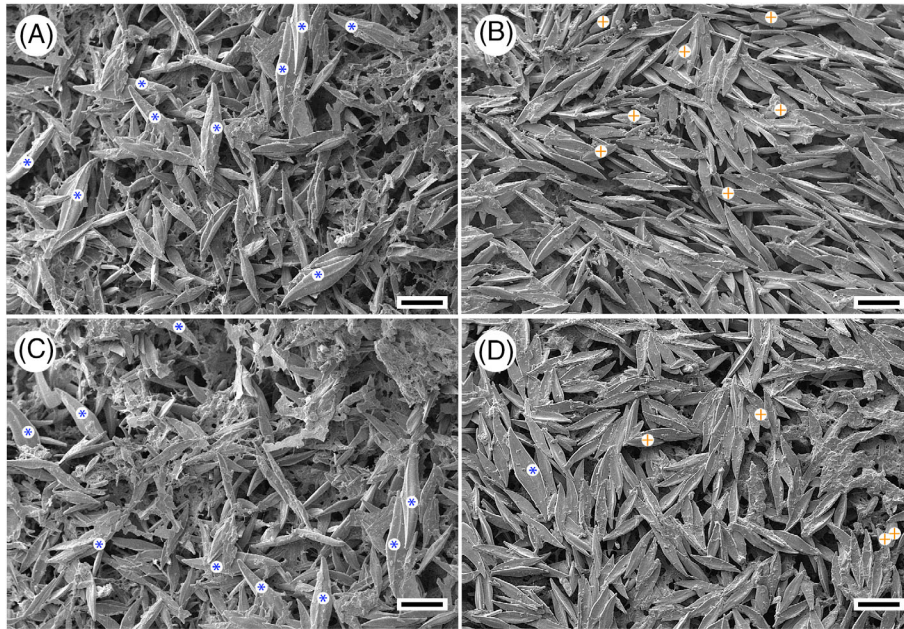


FIGURE 2 Low temperature scanning electron micrographs (LTSEM) of biofilms exposed to low light (A and C; $70 \mu\text{mol photons m}^{-2} \text{s}^{-1}$) and exposed to high light (B and D; $1000 \mu\text{mol photons m}^{-2} \text{s}^{-1}$). Blue stars indicate the presence of *Pleurosigma angulatum* and orange crosses the presence of *Plagiotropis neovitreia*. Scale bars: $100 \mu\text{m}$.

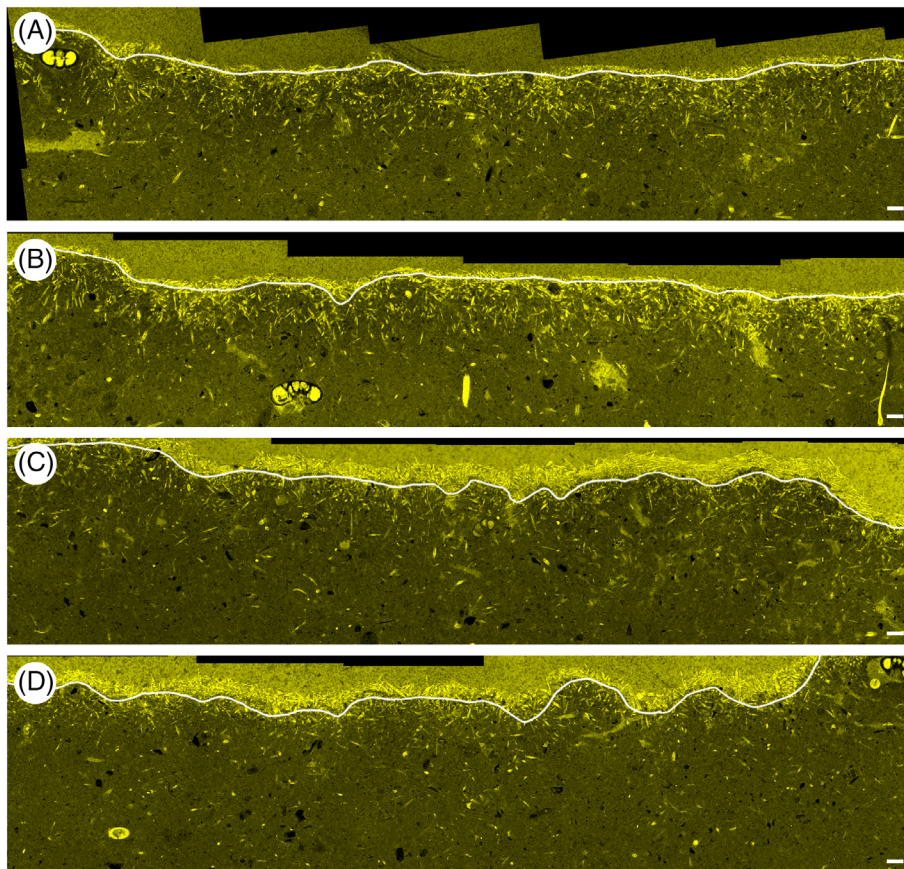


FIGURE 3 Fluorescently labelled embedded core (FLEC) images of the biofilm exposed to high light (A and B; $1000 \mu\text{mol photons m}^{-2} \text{s}^{-1}$) and exposed to low light (C and D; $70 \mu\text{mol photons m}^{-2} \text{s}^{-1}$). White line indicates the sediment surface. Scale bars: $100 \mu\text{m}$.

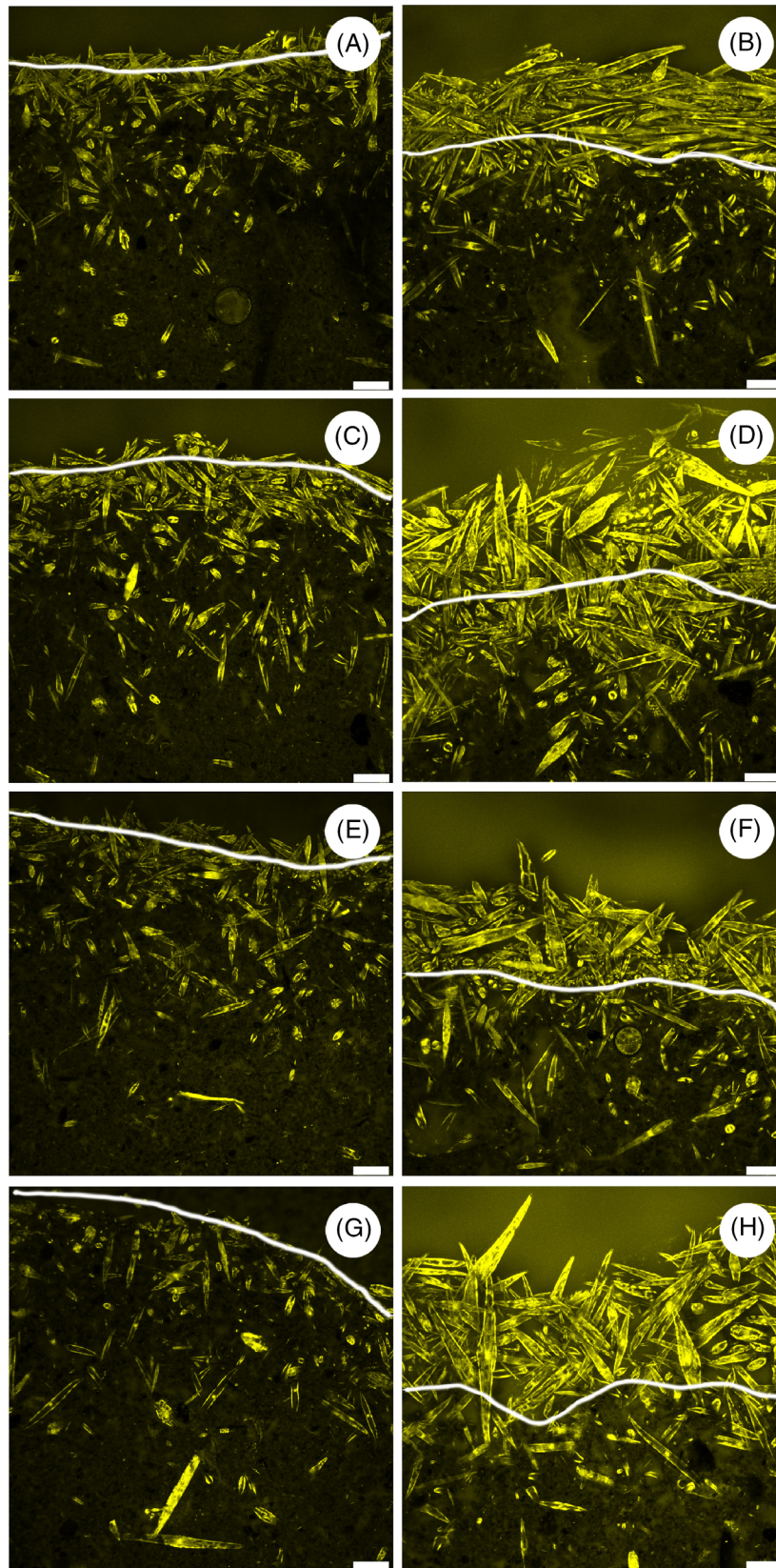


FIGURE 4 Fluorescently labelled embedded core (FLEC) detail images of the biofilm exposed to high light (A, C, E and G; $1000 \mu\text{mol photons m}^{-2} \text{s}^{-1}$) and exposed to low light (B, D, F and H; $70 \mu\text{mol photons m}^{-2} \text{s}^{-1}$). White line indicates the sediment surface. Scale bars: $50 \mu\text{m}$.

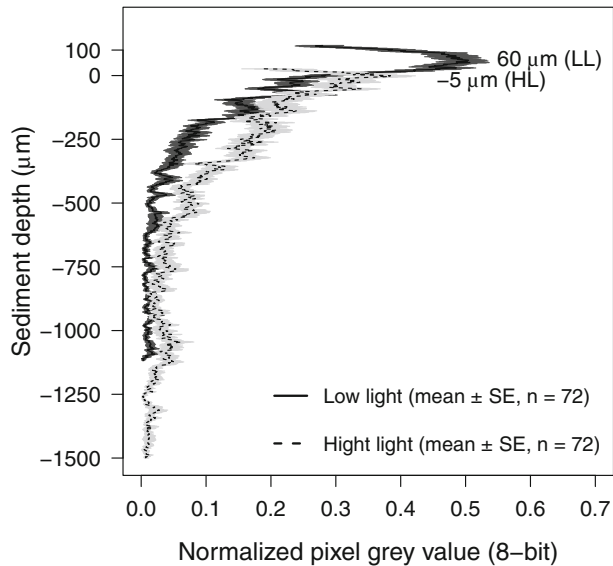


FIGURE 5 Vertical profiles of pixels with diatoms (normalized pixel grey value). Lines represent means and grey colours represent the standard error around the mean. $n = 72$. The two values in the graph represent the peaks for each treatment, $60 \mu\text{m}$ and $-5 \mu\text{m}$ for LL and HL, respectively.

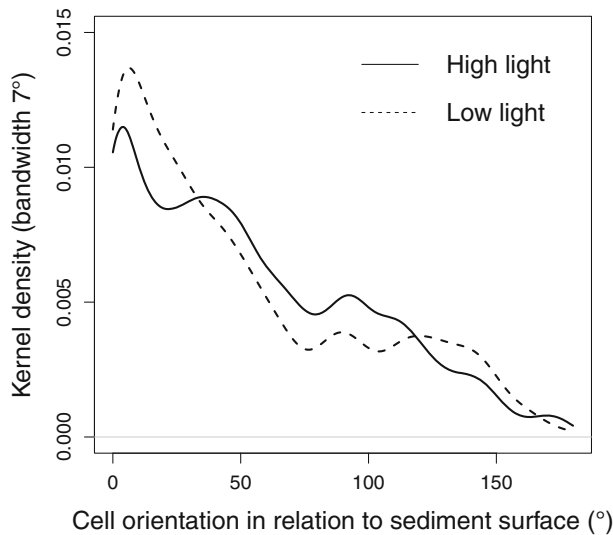


FIGURE 6 Kernel density curves of diatom cell orientation (in degrees) in relation to the surface, 0° and 180° represent a cell parallel to the surface and 90° represent a cell perpendicular to the sediment surface. $n = 644$ for LL and $n = 670$ for HL.

between all species ($p < 0.05$; Figure 8D) with the exception of the two *Pleurosigma* species. *Plagiotropis neovitre* showed the highest $rETR_{\text{max}}$ values while the *Pleurosigma* species showed the lowest values ($p < 0.05$; Figure 8D). NPQ values observed at the highest actinic light levels ($410 \mu\text{mol photons m}^{-2} \text{s}^{-1}$; 450 nm) were significantly different for all species ($p < 0.05$) with the two *Pleurosigma* species showing the highest values.

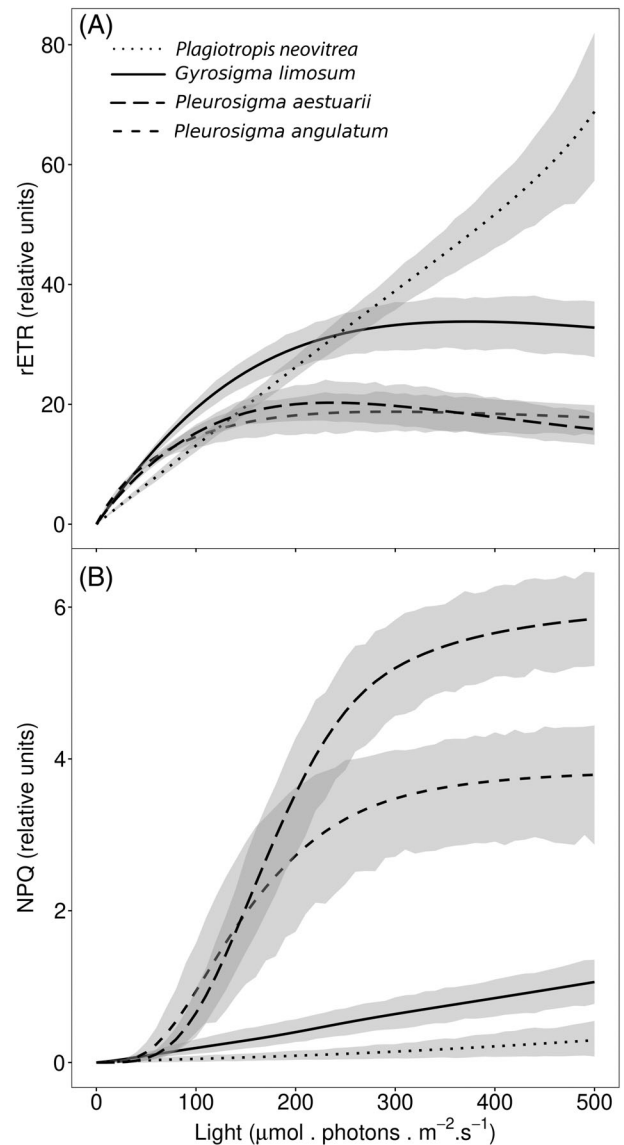


FIGURE 7 Rapid light curve (RLC) responses of *Plagiotropis neovitre*, *Gyrosigma limosum*, *Pleurosigma aestuarii* and *Pleurosigma angulatum*. Relative electron transport rate (rETR) in the top panel and non-photochemical quenching (NPQ) in the bottom panel. Lines are the mean values from the model estimations and the grey areas represent the 95% confidence interval estimated from bootstrap.

Among the four studied diatom species, *Plagiotropis neovitre* exhibited typical features of being acclimated to higher light levels, i.e., the lowest α value, a higher E_k value and the highest $rETR_{\text{max}}$ value (Figure 8B,D). In contrast both *Pleurosigma* sp. showed features of being acclimated to lower light levels as indicated by their lower E_k values and higher α values (Figure 8A,B).

Species-specific photo-acclimation responses were further supported by the light stress induction and recovery experiments (Figure 9). Here the PSII quantum yield of both *Pleurosigma aestuarii* and *Gyrosigma*

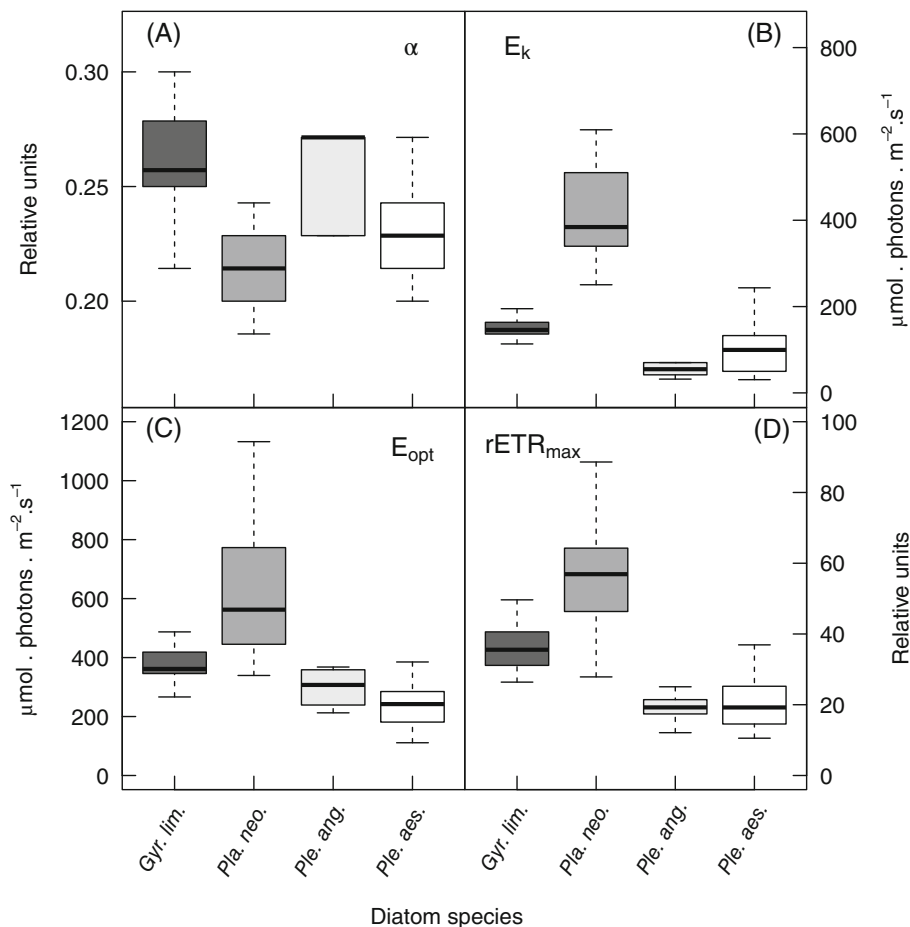


FIGURE 8 Rapid light curve (RLC) parameters for *Gyrosigma limosum*, *Plagiotropis neovitrea*, *Pleurosigma angulatum* and *Pleurosigma aestuarii*. (A) α , initial slope of the RLC at limiting irradiance. (B) E_k , light saturation coefficient. (C) E_{opt} , light at which rETR is maximal. (D) $r\text{ETR}_{\text{max}}$, maximum relative electron transport rate.

limosum decreased close to zero during the first minutes of light stress. However, while *P. aestuarii* recovered during the light stress and showed increasing YII values reaching ~20% of their original values, the YII of *G. limosum* only recovered 15% and even slightly decreased to 10% at the end of the light stress treatment (Figure 9A). At the end of the dark recovery period, YII of *P. aestuarii* did not recover fully to its original value ($p < 0.05$), albeit being close to a 100% recovery (97%) and significantly higher than in *G. limosum*, which showed incomplete recovery to ~47% of the initial average values ($p < 0.01$) (Figure 9A). The variability in *G. limosum* Y(II) recovery was also much more pronounced than that of *P. aestuarii* (Figure 9A).

Non-regulated energy dissipation, Y(NO), showed a sharp peak during the transition to light in both species but showed significant difference ($p < 0.01$) at the end of the light period they; decreasing almost to zero in *P. aestuarii* and never dropping below 23% in *G. limosum* (Figure 9B). At the end of the dark recovery period, Y(NO) showed significant differences between the two species ($p < 0.05$), with *P. aestuarii* values

recovering to their original values ($p > 0.05$) and *G. limosum* not recovering ($p < 0.05$) (Figure 9B). The Y(NPQ) values increased quickly for both species during the light stress, but at the end of light period the values were significantly higher ($p < 0.05$) for *P. aestuarii* (Figure 9C). During the dark recovery period, *P. aestuarii* NPQ values returned to their original values ($p > 0.05$), while *G. limosum* showed an initial steep decrease but then no change from 45% until the end of the recovery period, being significantly higher than their original values (Figure 9C).

DISCUSSION

Epipelagic diatoms are usually considered to be low light acclimated and having lower NPQ capability in comparison to epipsammic diatoms (Barnett et al., 2015; Blommaert et al., 2017, 2018; Jesus et al., 2009). However, our results show that diatoms within the same epipelagic biofilm exhibit species-specific photo-regulation responses and different acclimation regimes, ranging from very low light to high light.

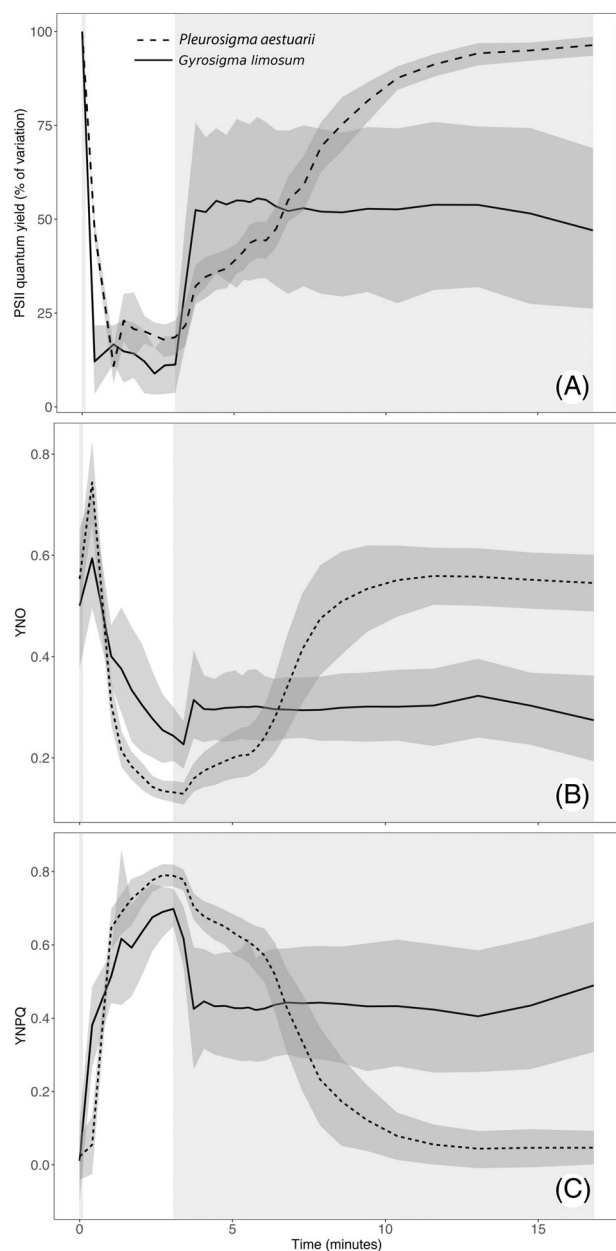


FIGURE 9 Induction recovery curves for *Pleurosigma aestuarii* ($n = 12$) and *Gyrosigma limosum* ($n = 6$). (A) PSII quantum efficiency (YII) variation from initial stage. (B) YNO, fraction of light energy that is dissipated via non-regulated mechanisms. (C) YNPQ, fraction of light energy that is dissipated by photo-protective regulated mechanisms. White areas represent the period of exposure to light, grey areas the dark exposure periods, lines are the means and the dark grey areas around the means represent 95% confidence intervals estimated from bootstrap.

Light induces complex diatom cell distributions in MPB

Exposing biofilms to high photon irradiance ($1000 \mu\text{mol photons m}^{-2} \text{s}^{-1}$; 400–700 nm) induced a clear downward vertical migration of the diatom biofilm into the sediment (Figure 3), similar to what has been

previously observed (Laviale et al., 2015; Laviale et al., 2016; Perkins et al., 2010; Serôdio et al., 2006). The movement response was very strong, with diatoms dispersing down to $\sim 500 \mu\text{m}$ below the sediment surface under HL, while a $\sim 100 \mu\text{m}$ thick diatom biofilm was observed on top of the sediment surface under LL (Figure 3). In situ photon irradiance (400–700 nm) at this latitude in April can easily reach more than $1000 \mu\text{mol photons m}^{-2} \text{s}^{-1}$ during low tide periods (Méléder et al., 2020). Therefore, for the majority of the species in the biofilm the in situ environmental light levels experienced at the sediment surface would be above the threshold that triggered the observed downward movement response. This suggests that most of the diatoms in the biofilm were acclimated to lower light than the maximum levels experienced at the sediment surface on a daily basis. Nevertheless, even at $1000 \mu\text{mol photons m}^{-2} \text{s}^{-1}$ there was always a layer of cells that stayed at the sediment surface. This indicates that some of our diatom species—or subpopulations of the same species—were better acclimated to high light and capable of photo-physiological acclimation without a need for moving away from excessive irradiance (Figure 3). This pattern might change with time given the dynamic nature of MPB movement response, namely, the dominant MPB species at the surface might change during the emersion cycle (Tolhurst et al., 2003; Underwood et al., 2005) or even exhibit microcycling at the sediment surface (Kromkamp et al., 1998). Temperature increases may also magnify the importance of photo-regulation vertical-response movements to light stress (Laviale et al., 2015).

Some diatom species have been shown to migrate to different depths according to their photo-acclimation level (Ezequiel et al., 2015). Our FLEC preparations revealed that not all diatoms migrated to a specific sediment horizon but were instead rather dispersed over a $\sim 500 \mu\text{m}$ wide depth interval (Figure 5). We speculate that this reflects differential acclimation of diatom species that distributed themselves in different depth horizons, accordingly. Also, it is possible that conspecific cells migrate to a depth range around their E_k value. It is highly likely that there are intra-specific variations in cell photo-acclimation parameters resulting in a range of E_k values rather than a single value. Thus, their depth distribution might reflect their range around the mean population E_k value. Assuming an average sediment light attenuation coefficient of 8.6 mm^{-1} (Cartaxana et al., 2011) and a surface photon irradiance of $1000 \mu\text{mol photons m}^{-2} \text{s}^{-1}$, diatom cells located at a depth of $500 \mu\text{m}$ would have been exposed to $13 \mu\text{mol photons m}^{-2} \text{s}^{-1}$ and cells at $100 \mu\text{m}$ would have been exposed to $110 \mu\text{mol photons m}^{-2} \text{s}^{-1}$. This illustrates the extreme light gradient experienced by epipelagic diatoms over very short distances and how most of the research done on laboratory cultures differs

considerably from the in situ conditions experienced by epipelagic diatoms. Barnett et al. (2015) grew cells at 20 and 75 $\mu\text{mol photons m}^{-2} \text{s}^{-1}$ for their LL and HL conditions, respectively, and Blommaert et al. (2018) grew cells at 20 $\mu\text{mol photons m}^{-2} \text{s}^{-1}$. In our biofilms, these light conditions would place their diatom cells at 450 μm and 300 μm deep for their LL and HL, respectively. This estimate is close to the lower limit of the cells we observed in our 1000 $\mu\text{mol photons m}^{-2} \text{s}^{-1}$ treatment, suggesting that all species in the studies of Barnett et al. (2015) and Blommaert et al. (2018) were acclimated to lower light conditions than the ones measured here.

FLEC was developed to reveal fine-scale distributions of metabolically active sediment-dwelling organisms, where they were living, at the time of fixation (Bernhard et al., 2003). The technique reveals undisturbed life positions of metazoans (Bernhard et al., 2023), protists (Bernhard et al., 2013) and larger bacteria (Bernhard et al., 2003) within the sedimentary matrix. Such attributes confer valuable information on entire benthic communities, for example, in Figure 3A,B,D—in addition to the diatom biofilm—living foraminifera can be seen below the biofilm. Benthic diatoms are common foraminiferal prey (Jesus et al., 2022). The FLEC approach is particularly well suited for MPB studies (First & Hollibaugh, 2010) because it labels active diatom cells, thereby distinguishing them from empty diatom frustules. Some studies have used LTSEM vertical profiles to investigate diatom cell distribution with depth (Kelly et al., 2001; Paterson, 1986; Taylor & Paterson, 1998; Wiltshire et al., 1997) but in most cases it is very difficult to separate the sediment matrix from the cells once the cells are dispersed deep in the sediment, and it is impossible to know which cells, if any, were viable. FLEC overcomes these issues, and combining FLEC confocal fluorescence images with SEM images makes it much easier to determine where the sediment surface is located in vertical profiles and therefore to estimate how deep cells have migrated (Figure S3).

LTSEM is still very useful to obtain information from the biofilm surface and has been frequently used to study biofilm changes at the sediment surface (Tolhurst et al., 2003; Underwood et al., 2005), but often it is difficult to obtain quantitative information of the species present at the sediment surface because it only detects the first cell layer, often hiding all the other cells underneath (Figure 4B). The main difference we observed in LTSEM images was the relative increase of *Pleurosigma angulatum* in comparison with *P. aestuarii* in the LL biofilm and the presence of *Plagiotropis neovitrea* in HL (Figure 2B,D, otherwise absent in the LL LTSEM samples (Figure 2A,C)). These differences were coherent with the counts done on cells collected by the lens tissue technique where we also observed a decrease in *P. angulatum* in the HL condition accompanied by an

increase in *Plagiotropis neovitrea* (Table 1). Cells counts also detected a decrease in *G. limosum* cells and an increase in *Pleurosigma aestuarii* in the HL conditions. This is the first indication that light response movements were species-specific.

Light level affects diatom cell orientation in MPB

Analysing whole biofilm movements with the FLEC technique confirmed that the biofilms migrated deeper into the sediment under HL (Figures 3 and 4), which is consistent with previous observations that excessive light induces photophobic movements (Cartaxana et al., 2011; Perkins et al., 2002; Perkins et al., 2010; Underwood et al., 2005). Additionally, the FLEC vertical profiles showed a clear difference in the biofilm structure, with cells in the LL condition forming a multilayered biofilm at the sediment surface (Figure 4) of cells oriented more parallel to the sediment surface; while the HL biofilm was mostly inside the sediment surface and with cells oriented more perpendicularly to the sediment surface (Figures 5 and 6). It is possible that cell orientation might have an important role in benthic diatom photo-regulation, as has, for example, also been proposed for cyanobacteria in hot spring microbial mats (Ramsing et al., 2000). Diatom cells parallel to the sediment surface would maximize the exposure of their chloroplasts to incident light and thus more likely to be observed in LL conditions, while cells positioned perpendicularly to the sediment would strongly reduce their absorption cross-section thus decreasing their light exposure and more likely to be observed in HL conditions.

Diatom frustules and live benthic diatoms have also been shown to work as photonic crystal-like structures that can increase forward blue light scattering (Goessling, Frankenbach, et al., 2018). This would be particularly useful in longer cells (e.g., *Pleurosigma* sp., *Gyrosigma* sp.) that could keep part of the cell inside the sediment and expose only one tip to ambient light, guiding light to the rest of the cell via increased forward light scattering or photon migration in the frustule (Goessling, Frankenbach, et al., 2018; Goessling, Su, et al., 2018). There is, however, little information about diatom cell orientation inside MPB. Jönsson et al. (1994) described a subtidal diatom biofilm dominated by *G. balticum* oriented vertically in the sediment and capable of vertical movements inside a short EPS tube, sometimes extending their cells outside the sediment. They reported these movements as a circadian response to day-night cycles, but they did not test if cells could adjust their position inside the EPS tube as a short-term photo-regulatory mechanism. Much more experimental work on the structural plasticity of MPB and mechanisms affecting cell migration and

orientation is needed. Namely, it would be immensely valuable to develop imaging techniques allowing the in situ measurement of photo-physiological parameters coupled with diatom movement response in structured biofilms.

Differential photo-acclimation facilitates coexistence of different epipellic diatoms

Variable chlorophyll fluorescence measurements as a function of photon irradiance are strong tools to characterize the photo-physiological light-acclimation status of diatoms, for example, by comparing E_k and NPQ values under different light scenarios (Barnett et al., 2015; Blommaert et al., 2017, 2018; Serôdio, Cruz, et al., 2005; Serôdio, Vieira, et al., 2005). In our study, all four epipellic diatom species showed clear differences in rETR and NPQ derived parameters (Figures 7 and 8). *Plagiotropis neovitrea* parameters consistently showed signs of acclimation to higher light levels, whereas the two *Pleurosigma* species showed signs of being acclimated to lower light levels than *Plagiotropis neovitrea* and sometimes to lower levels than *G. limosum* that showed inconclusive photo-acclimation status in comparison to the other diatom species.

The NPQ data was significantly different for all diatom species (Figure 7B), with saturation and high NPQ values found in the two *Pleurosigma* species in comparison to the other two species that showed low NPQ values and no sign of saturation. We note that NPQ data derived from RLC measurements are complex to interpret because the rapid light steps (20 s in our case) might be insufficient to fully convert the xanthophyll pigments responsible for the majority of diatom NPQ response (Jesus et al., 2008). A linear interpretation of Figure 7B would point to the two *Pleurosigma* species being acclimated to high light and *Plagiotropis neovitrea* and *G. limosum* to lower light. However, the low NPQ values of *G. limosum* and *P. neovitrea* might have different origins. The cell count analysis points to *P. neovitrea* being more HL adapted than all the other species since it was more frequent in the HL samples. Thus, it is possible that *P. neovitrea* NPQ was still in the lag stage at $500 \mu\text{mol photons m}^{-2} \text{s}^{-1}$ and eventually, given more light, they would start to increase NPQ to quench excessive energy. In contrast, *G. limosum* might be low light adapted and not capable of reaching much higher NPQ levels than the ones observed; this would, for example, be coherent with its higher a values (Figure 8) and with the observation that when exposed to light stress for longer periods *G. limosum* was not as resilient as *P. aestuarii* (Figure 9). The different photo-acclimation levels exhibited by the two species might result from different genetic constraints impacting their acclimation range; further experimental studies are needed to confirm this possibility.

The induction-recovery experiment (Figure 9) showed clear differences between *P. aestuarii* and *G. limosum*, with the latter showing strong signs of being acclimated to lower light levels than the former. Namely, during the light stress *G. limosum* showed lower PSII efficiency, lower NPQ capacity and higher Y(NO) values. This was further corroborated by the lack of recovery to the initial values at the end of the recovery period and much higher variability (Figure 9). Nevertheless, *G. limosum* was capable of reaching higher NPQ values than the ones observed in the short 20-s RLC steps (Figures 7 and 9).

There is little information on species-specific responses in the photo-acclimation of diatoms in MPB. Overall, we obtained similar results as Underwood et al. (2005), who observed that *Pleurosigma angulatum* preferred higher light conditions than *G. balticum*, which was clearly low light acclimated. They also observed a *Plagiotropis* species, that is, *Plagiotropis vitrea*, which is closely related to the *Plagiotropis neovitrea* in our study (Paddock, 1988). However, the behaviour of the two species was different, with *Plagiotropis vitrea* moving away from high light, while in our study *Plagiotropis neovitrea* preferred high light. Underwood et al. (2005) reported that *Pleurosigma angulatum* from two different sites exhibited different PSII quantum efficiencies. Barnett et al. (2015) reported epipellic diatoms with maximum NPQ values around 0.5 and epipsammic species reaching NPQ values of around 2.5. This contrast with our observations that epipellic species from the same biofilm can exhibit very different maximum NPQ values. In our case, the maximum NPQ values ranged from 0.3 in *Plagiotropis neovitrea* to 5.8 in *Pleurosigma aestuarii*, the latter being more than double of the values observed by Barnett et al. (2015) for epipsammic species. Thus, it is likely that different populations of the same diatom species, or closely related species, can have a different photo-acclimation status that depends on their light history.

Overall, our results show that different species from the same epipellic biofilm can exhibit different photo-acclimation status, which could facilitate their coexistence in the photic zone of muddy sediments. This would be a highly efficient mechanism for niche separation inside a light gradient, similar to phytoplankton observations in stratified waters (Moore et al., 2006). However, phytoplankton light gradients operate at a metric scale, while microphytobenthos light gradients in the sediment change dramatically over μm scales, creating extremely steep gradients with depth. For example, in the HL condition and using a typical light attenuation coefficient of 8.6 mm^{-1} in muddy sediments (Cartaxana et al., 2011), a $260 \mu\text{m}$ long *P. angulatum* cell oriented vertically in the sediment would be exposed to $1000 \mu\text{mol photons m}^{-2} \text{s}^{-1}$ in one tip and $105 \mu\text{mol photons m}^{-2} \text{s}^{-1}$ at the other tip. Thus, even small vertical movements would expose the cell to a radically different light environment. Although not

specifically investigated in our study, the counter argument could be made for epipsammic diatoms; at 1000 $\mu\text{mol photons m}^{-2} \text{s}^{-1}$ a sandy sediment with a light attenuation coefficient of 1.6 mm^{-1} (Cartaxana et al., 2011) at the same distance of 260 μm light will only be attenuated to 660 $\mu\text{mol photons m}^{-2} \text{s}^{-1}$. The average length of epipsammic species is 7–10 μm (Jesus et al., 2009), thus, they will not experience a strong light gradient at their cell-size scale and it could be argued that they live in more predictable light environments (Paterson et al., 2009). However, sandy sediments are characteristic of more variable hydrodynamic conditions, leading to increased remixing of the sediment matrix (Paterson et al., 2009). Diatom cells colonizing sand grains at the sediment surface might thus be relocated to deeper sediments between tidal cycles, thereby experiencing a more dynamic and unpredictable light regime. Therefore, even if, overall, photo-physiological traits can sometimes be generalized between natural epipsammic and epipelagic communities (Cartaxana et al., 2011; Jesus et al., 2009) more studies are needed on the species-specific responses of benthic diatoms grown at light conditions similar to the ones experienced in nature, preferably coupling their photo-physiology with behavioural-movement response.

CONCLUSION

Benthic diatoms experience extreme light gradients over very short (μm) distances. Nevertheless, several diatom species can coexist in dense biofilms at the sediment–water interface. We tested the hypothesis that epipelagic diatoms are typically low light acclimated due to their capacity to migrate within such light gradients. We show that diatoms from the same biofilm exhibit species-specific photo-regulation responses and can have very different acclimation regimes. This would allow different species with the same growth-form, that is, epipelagic motile diatoms, to coexist in the compacted light niche of MPB communities. We also show that cell orientation within diatom biofilms can be modulated by light, where diatoms oriented themselves more perpendicular to the sediment surface under high light, and more parallel to the surface under low light. Besides the well-established vertical migration patterns of diatoms, cell orientation could be another behavioural, photo-regulatory response of diatoms enabling them to vary their light absorption cross-section. Overall, the results improve our understanding of the complex ecological dynamics of microalgal biofilms and highlight the importance of considering species-specific responses and understanding cell orientation in response to light, especially in MPB research.

AUTHOR CONTRIBUTIONS

Bruno Jesus: Conceptualization (equal); data curation (lead); formal analysis (equal); funding acquisition (equal); investigation (equal); methodology (equal); resources (equal); validation (equal); visualization (equal); writing – original draft (lead); writing – review and editing (equal). **Thierry Jauffrais:** Conceptualization (equal); data curation (supporting); formal analysis (supporting); investigation (equal); methodology (equal); validation (equal); writing – original draft (supporting); writing – review and editing (equal). **Erik Trampe:** Formal analysis (supporting); investigation (supporting); methodology (supporting); resources (supporting); validation (supporting); writing – review and editing (supporting). **Vona Meleder:** Formal analysis (supporting); investigation (supporting); methodology (supporting); validation (supporting); writing – review and editing (supporting). **Lourenço Ribeiro:** Data curation (supporting); formal analysis (supporting); methodology (supporting); visualization (supporting); writing – review and editing (supporting). **Joan M. Bernhard:** Formal analysis (supporting); methodology (supporting); supervision (supporting); validation (supporting); writing – review and editing (supporting). **Emmanuelle Geslin:** Funding acquisition (equal); methodology (supporting); project administration (equal); resources (supporting); supervision (supporting); writing – review and editing (supporting). **Michael Kühl:** Conceptualization (supporting); funding acquisition (equal); methodology (equal); project administration (equal); resources (equal); supervision (equal); validation (equal); writing – original draft (supporting); writing – review and editing (supporting).

ACKNOWLEDGEMENTS

TJ was funded by the ‘FRESCO’ project supported by the Region Pays de Loire and the University of Angers. The authors thank the SCIAM imaging facility at the University of Angers (France) where the confocal, SEM and cryo-SEM images were produced with the help of Rodolphe Perrot and Romain Mallet, respectively. MK acknowledges financial support from the Independent Research Fund Denmark (DFF-8022-00301B). JMB acknowledges support from WHOI’s Investment in Science Program. BJ acknowledges support by the European Union’s Horizon 2020 research and innovation programme under the Marie Skłodowska-Curie grant agreement N° 860125. We thank the three reviewers for their insights.

CONFLICT OF INTEREST STATEMENT


The authors have no conflict of interest to declare.

DATA AVAILABILITY STATEMENT

Data available on request from the authors.

ORCID

Bruno Jesus  <https://orcid.org/0000-0002-2047-3783>

Thierry Jauffrais  <https://orcid.org/0000-0001-9681-6239>

Michael Kühl  <https://orcid.org/0000-0002-1792-4790>

REFERENCES

- Admiraal, W. (1984) The ecology of estuarine sediment-inhabiting diatoms. *Progress in Phycological Research*, 3, 269–322.
- Barnett, A., Méléder, V., Blommaert, L., Lepetit, B., Gaudin, P., Vyverman, W. et al. (2015) Growth form defines physiological photoprotective capacity in intertidal benthic diatoms. *The ISME Journal*, 9, 32–45.
- Bernhard, J.M. & Bowser, S.S. (1996) Novel epifluorescence microscopy method to determine life position of foraminifera in sediments. *Journal of Micropalaeontology*, 15, 68.
- Bernhard, J.M., Edgcomb, V.P., Visscher, P.T., McIntyre-Wressnig, A., Summons, R.E., Bousein, M.L. et al. (2013) Insights into foraminiferal influences on microfibrils of microbialites at Highborne Cay, Bahamas. *Proceedings of the National Academy of Sciences of the United States of America*, 110, 9830–9834.
- Bernhard, J.M., Nomaki, H., Shiratori, T., Elmendorf, A., Yabuki, A., Kimoto, K. et al. (2023) Hydrothermal vent chimney-base sediments as unique habitat for meiobenthos and nanobenthos: observations on millimeter-scale distributions. *Frontiers in Marine Science*, 9, 1033381. Available from: <https://doi.org/10.3389/fmars.2022.1033381>
- Bernhard, J.M., Visscher, P.T. & Bowser, S.S. (2003) Submillimeter life positions of bacteria, protists, and metazoans in laminated sediments of the Santa Barbara Basin. *Limnology and Oceanography*, 48, 813–828.
- Blommaert, L., Chafai, L. & Bailleul, B. (2021) The fine-tuning of NPQ in diatoms relies on the regulation of both xanthophyll cycle enzymes. *Scientific Reports*, 11, 12750.
- Blommaert, L., Huysman, M., Vyverman, W., Lavaud, J. & Sabbe, K. (2017) Contrasting NPQ dynamics and xanthophyll cycling in a motile and a non-motile intertidal benthic diatom. *Limnology and Oceanography*, 62, 1466–1479.
- Blommaert, L., Lavaud, J., Vyverman, W. & Sabbe, K. (2018) Behavioural versus physiological photoprotection in epipelagic and epipsammic benthic diatoms. *European Journal of Phycology*, 53, 146–155.
- Brotas, V., Risgaard-Petersen, N., Serôdio, J., Ottosen, L., Dalsgaard, T. & Ribeiro, L. (2003) *In situ* measurements of photosynthetic activity and respiration of intertidal benthic microalgal communities undergoing vertical migration. *Ophelia*, 57, 13–26.
- Cabrita, M.T. & Brotas, V. (2000) Seasonal variation in denitrification and dissolved nitrogen fluxes in intertidal sediments of the Tagus estuary, Portugal. *Marine Ecology Progress Series*, 202, 51–65.
- Cartaxana, P., Domingues, N., Cruz, S., Jesus, B., Laviale, M., Serôdio, J. et al. (2013) Photoinhibition in benthic diatom assemblages under light stress. *Aquatic Microbial Ecology*, 70, 87–92.
- Cartaxana, P., Ribeiro, L., Goessling, J.W., Cruz, S. & Kühl, M. (2016) Light and O₂ microenvironments in two contrasting diatom-dominated coastal sediments. *Marine Ecology Progress Series*, 545, 35–47.
- Cartaxana, P., Ruivo, M., Hubas, C., Davidson, I., Serôdio, J. & Jesus, B. (2011) Physiological versus behavioral photoprotection in intertidal epipelagic and epipsammic benthic diatom communities. *Journal of Experimental Marine Biology and Ecology*, 405, 120–127.
- Cartaxana, P. & Serôdio, J. (2008) Inhibiting diatom motility: a new tool for the study of the photophysiology of intertidal microphytobenthic biofilms. *Limnology and Oceanography: Methods*, 6, 466–476.
- Cruz, S. & Serôdio, J. (2008) Relationship of rapid light curves of variable fluorescence to photoacclimation and non-photochemical quenching in a benthic diatom. *Aquatic Botany*, 88, 256–264.
- Derks, A.K. & Bruce, D. (2018) Rapid regulation of excitation energy in two pennate diatoms from contrasting light climates. *Photosynthesis Research*, 138, 149–165.
- Dong, L.F., Thornton, D.C.O., Nedwell, D.B. & Underwood, G.J.C. (2000) Denitrification in sediments of the river Colne estuary, England. *Marine Ecology Progress Series*, 203, 109–122.
- Eaton, J.W. & Moss, B. (1966) The estimation of numbers and pigment content in epipelagic algal populations. *Limnology and Oceanography*, 11, 584–595.
- Eilers, P.H.C. & Peeters, J.C.H. (1988) A model for the relationship between light intensity and the rate of photosynthesis in phytoplankton. *Ecological Modelling*, 42, 199–215.
- Ezequiel, J., Laviale, M., Frankenbach, S., Cartaxana, P. & Serôdio, J. (2015) Photoacclimation state determines the photo-behaviour of motile microalgae: the case of a benthic diatom. *Journal of Experimental Marine Biology and Ecology*, 468, 11–20.
- First, M.R. & Hollibaugh, J.T. (2010) Diel depth distributions of microbenthos in tidal creek sediments: high resolution mapping in fluorescently labeled embedded cores. *Hydrobiologia*, 655, 149–158.
- Frankenbach, S., Ezequiel, J., Plecha, S., Goessling, J.W., Vaz, L., Kühl, M. et al. (2020) Synoptic spatio-temporal variability of the photosynthetic productivity of microphytobenthos and phytoplankton in a tidal estuary. *Frontiers in Marine Science*, 7, 170.
- Glud, R.N., Woelfel, J., Karsten, U., Kühl, M. & Rysgaard, S. (2009) Benthic microalgal production in the Arctic: applied methods and status of the current database. *Botanica Marina*, 52, 559–571.
- Goessling, J.W., Frankenbach, S., Ribeiro, L., Serôdio, J. & Kühl, M. (2018) Modulation of the light field related to valve optical properties of raphid diatoms: implications for niche differentiation in the microphytobenthos. *Marine Ecology Progress Series*, 588, 29–42.
- Goessling, J.W., Su, Y., Cartaxana, P., Maibohm, C., Rickelt, L.F., Trampe, E. et al. (2018) Structure-based optics of centric diatom frustules: modulation of the *in vivo* light field for efficient diatom photosynthesis. *The New Phytologist*, 219, 122–134.
- Hope, J.A., Paterson, D.M. & Thrush, S.F. (2019) The role of microphytobenthos in soft-sediment ecological networks and their contribution to the delivery of multiple ecosystem services. *Journal of Ecology*, 108, 815–830.
- Jesus, B., Brotas, V., Ribeiro, L., Mendes, C.R., Cartaxana, P. & Paterson, D.M. (2009) Adaptations of microphytobenthos assemblages to sediment type and tidal position. *Continental Shelf Research*, 29, 1624–1634.
- Jesus, B., Jauffrais, T., Trampe, E.C.L., Goessling, J.W., Lekieffre, C., Meibom, A. et al. (2022) Kleptoplast distribution, photosynthetic efficiency and sequestration mechanisms in intertidal benthic foraminifera. *The ISME Journal*, 16, 822–832.
- Jesus, B., Mouget, J.-L. & Perkins, R.G. (2008) Detection of diatom xanthophyll cycle using spectral reflectance. *Journal of Phycology*, 44, 1349–1359.
- Jesus, B., Perkins, R.G., Mendes, C.R., Brotas, V. & Paterson, D.M. (2006) Chlorophyll fluorescence as a proxy for microphytobenthic biomass: alternatives to the current methodology. *Marine Biology*, 150, 17–28.
- Jönsson, B., Sundbäck, K. & Nilsson, C. (1994) An upright life-form of an epipelagic motile diatom: on the behaviour of *Gyrosigma balticum*. *European Journal of Phycology*, 29, 11–15.
- Kelly, J., Honeywill, C. & Paterson, D. (2001) Microscale analysis of chlorophyll-a in cohesive, intertidal sediments: the implications of microphytobenthos distribution. *Journal of the Marine Biological Association of the United Kingdom*, 81, 151–162.
- Klughammer, C. & Schreiber, U. (2008) Complementary PSII quantum yields calculated from simple fluorescence parameters

- measured by PAM fluorometry and the saturation pulse method. *PAM Application Notes*, 1, 27–35.
- Kromkamp, J., Barranguet, C. & Peene, J. (1998) Determination of microphytobenthos PSII quantum efficiency and photosynthetic activity by means of variable chlorophyll fluorescence. *Marine Ecology Progress Series*, 162, 45–55.
- Kühl, M. & Jørgensen, B.B. (1994) The light field of micro-benthic communities: radiance distribution and microscale optics of sandy coastal sediments. *Limnology and Oceanography*, 39, 1368–1398.
- Lavaud, J., Rousseau, B., van Gorkom, H.J. & Etienne, A.L. (2002) Influence of the diadinoxanthin pool size on photoprotection in the marine planktonic diatom *Phaeodactylum tricornutum*. *Plant Physiology*, 129, 1398–1406.
- Laviale, M., Barnett, A., Ezequiel, J., Lepetit, B., Frankenbach, S., Méléder, V. et al. (2015) Response of intertidal benthic microalgal biofilms to a coupled light-temperature stress: evidence for latitudinal adaptation along the Atlantic coast of southern Europe. *Environmental Microbiology*, 17, 3662–3677.
- Laviale, M., Frankenbach, S. & Serôdio, J. (2016) The importance of being fast: comparative kinetics of vertical migration and non-photochemical quenching of benthic diatoms under light stress. *Marine Biology*, 163, 10.
- Lefebvre, S., Mouget, J.-L. & Lavaud, J. (2011) Duration of rapid light curves for determining the photosynthetic activity of microphytobenthos biofilm *in situ*. *Aquatic Botany*, 95, 1–8.
- MacIntyre, H.L., Geider, R.J. & Miller, D.C. (1996) Microphytobenthos: the ecological role of the “secret garden” of unvegetated, shallow-water marine habitats. I. Distribution, abundance and primary production. *Estuaries*, 19, 186–201.
- McIntire, C.D. & Moore, W.W. (1977) Marine littoral diatoms: ecological considerations. In: Werner, D. (Ed.) *The biology of diatoms*. Oxford: Blackwell Scientific Publications, pp. 333–371.
- Méléder, V., Jesus, B., Barnett, A., Barillé, L. & Lavaud, J. (2018) Microphytobenthos primary production estimated by hyperspectral reflectance. *PLoS One*, 13(5), e0197093.
- Méléder, V., Rincé, Y., Barillé, L., Gaudin, P. & Rosa, P. (2007) Spatiotemporal changes in microphytobenthos assemblages in a macrotidal flat (Bourgneuf Bay, France). *Journal of Phycology*, 43, 1177–1190.
- Méléder, V., Savelli, R., Barnett, A., Polsenaere, P., Gernez, P., Cugier, P. et al. (2020) Mapping the intertidal microphytobenthos gross primary production part I: coupling multispectral remote sensing and physical modeling. *Frontiers in Marine Science*, 7, 520.
- Middelburg, J.J., Barranguet, C., Boschker, H.T.S., Herman, P.M.J., Moens, T. & Heip, C.H.R. (2000) The fate of intertidal microphytobenthos carbon: an *in situ* ^{13}C labelling study. *Limnology and Oceanography*, 45, 1224–1234.
- Moore, C.M., Suggett, D.J., Hickman, A.E., Kim, Y.-N., Tweddle, J.F., Sharples, J. et al. (2006) Phytoplankton photoacclimation and photoadaptation in response to environmental gradients in a shelf sea. *Limnology and Oceanography*, 51, 936–949.
- Paddock, T.B.B. (1988) *Plagiotropis Pfitzer and Tropidoneis Cleve, a summary account*. Berlin-Stuttgart: J. Cramer, pp. 1–190.
- Paterson, D.M. (1986) The migratory behaviour of diatom assemblages in a laboratory tidal micro-ecosystem examined by low-temperature scanning electron microscopy. *Diatom Research*, 1, 227–239.
- Paterson, D.M. (1989) Short-term changes in the erodibility of intertidal cohesive sediments related to the migratory behaviour of epipelagic diatoms. *Limnology and Oceanography*, 34, 223–234.
- Paterson, D.M., Aspden, R.J. & Black, K.S. (2009) Intertidal flats: ecosystem functioning of soft sediment systems. In: Perillo, G.M.E., Wolanski, E., Cahoon, D.R. & Brinson, M.M. (Eds.) *Coastal wetlands: an integrated ecosystem approach*. Netherlands: Elsevier, pp. 317–338.
- Perkins, R.G., Lavaud, J., Serôdio, J., Mouget, J.L., Cartaxana, P., Rosa, P. et al. (2010) Vertical cell movement is a primary response of intertidal benthic biofilms to increasing light dose. *Marine Ecology Progress Series*, 416, 93–103.
- Perkins, R.G., Oxborough, K., Hanlon, A.R.M., Underwood, G.J.C. & Baker, N.R. (2002) Can chlorophyll fluorescence be used to estimate the rate of photosynthetic electron transport within microphytobenthic biofilms? *Marine Ecology Progress Series*, 228, 47–56.
- Perkins, R.G., Underwood, G.J.C., Brotas, V., Snow, G.C., Jesus, B. & Ribeiro, L. (2001) Responses of microphytobenthos to light: primary production and carbohydrate allocation over an emersion period. *Marine Ecology Progress Series*, 223, 101–112.
- Pinckney, J.L. (2018) A mini-review of the contribution of benthic microalgae to the ecology of the continental shelf in the South Atlantic bight. *Estuaries and Coasts*, 41, 2070–2078.
- Prins, A., Deleris, P., Hubas, C. & Jesus, B. (2020) Effect of light intensity and light quality on diatom behavioral and physiological photoprotection. *Frontiers in Marine Science*, 7, 203. Available from: <https://doi.org/10.3389/fmars.2020.00203>
- R Core Team. (2020) *R: a language and environment for statistical computing*. Vienna, Austria: R Foundation for Statistical Computing. Available from: <https://www.R-project.org/>
- Ralph, P.J. & Gademann, R. (2005) Rapid light curves: a powerful tool to assess photosynthetic activity. *Aquatic Botany*, 82, 222–237.
- Ramsing, N.B., Ferris, M.J. & Ward, D.M. (2000) Highly ordered vertical structure of *Synechococcus* populations within the one-millimeter thick photic zone of a hot spring cyanobacterial mat. *Applied and Environmental Microbiology*, 66, 1038–1049.
- Ribeiro, L., Benyoucef, I., Poulin, M., Jesus, B., Rosa, P., Méléder, V. et al. (2021) Spatio-temporal variation of microphytobenthos biomass, diversity and assemblage structure in the Loire estuary, France. *Aquatic Microbial Ecology*, 87, 61–77.
- Ribeiro, L., Brotas, V., Rincé, Y. & Jesus, B. (2013) Structure and diversity of intertidal benthic diatom assemblages in contrasting shores: a case study from the Tagus estuary. *Journal of Phycology*, 49, 258–270.
- Rivera-Garcia, L.G., Hill-Spanik, K.M., Berthrong, S.T. & Plante, C.J. (2017) Tidal stage changes in structure and diversity of intertidal benthic diatom assemblages: a case study from two contrasting Charleston Harbor flats. *Estuaries and Coasts: Journal of the Estuarine Research Federation*, 41, 772–783.
- Round, F.E. (1971) Marine benthic diatoms. In: Barnes, H. (Ed.) *Oceanography and marine biology annual review*. London: George Allen & Unwin Ltd, pp. 83–139.
- Ruban, A., Lavaud, J., Rousseau, B., Guglielmi, G., Horton, P. & Etienne, A.-L. (2004) The super-excess energy dissipation in diatom algae: comparative analysis with higher plants. *Photosynthesis Research*, 82, 165–175.
- Sabbe, K. (1997) *Systematics and ecology of intertidal benthic diatoms of the Westerschelde estuary (The Netherlands)*. PhD thesis. Belgium: Universiteit Gent.
- Schneider, C.A., Rasband, W.S. & Eliceiri, K.W. (2012) NIH image to ImageJ: 25 years of image analysis. *Nature Methods*, 9, 671–675.
- Schreiber, U., Schliwa, U. & Bilger, W. (1986) Continuous recording of photochemical and non-photochemical chlorophyll fluorescence quenching with a new type of modulation fluorometer. *Photosynthesis Research*, 10, 51–62.
- Serôdio, J. & Catarino, F. (1999) Fortnightly light and temperature variability in estuarine intertidal sediments and implications for microphytobenthos primary productivity. *Aquatic Ecology*, 33, 235–241.
- Serôdio, J., Coelho, H., Vieira, S. & Cruz, S. (2006) Microphytobenthos vertical migratory photoresponse as characterised by

- light-response curves of surface biomass. *Estuarine, Coastal and Shelf Science*, 68, 547–556.
- Serôdio, J., Cruz, S., Vieira, S. & Brotas, V. (2005) Non-photochemical quenching of chlorophyll fluorescence and operation of the xanthophyll cycle in estuarine microphytobenthos. *Journal of Experimental Marine Biology and Ecology*, 326, 157–169.
- Serôdio, J. & Lavaud, J. (2011) A model for describing the light response of the nonphotochemical quenching of chlorophyll fluorescence. *Photosynthesis Research*, 108, 61–76.
- Serôdio, J., Marques da Silva, J. & Catarino, F. (1997) Non-destructive tracing of migratory rhythms of intertidal benthic microalgae using *in vivo* chlorophyll *a* fluorescence. *Journal of Phycology*, 33, 542–553.
- Serôdio, J. & Paterson, D.M. (2020) Role of microphytobenthos in the functioning of estuarine and coastal ecosystems. In: Leal Filho, W., Azul, A.M., Brandli, L., Lange Salvia, A. & Wall, T. (Eds.) *Life below water*. Switzerland: Springer International Publishing, pp. 1–13.
- Serôdio, J., Vieira, S., Cruz, S. & Barroso, F. (2005) Short-term variability in the photosynthetic activity of microphytobenthos as detected by measuring rapid light curves using variable fluorescence. *Marine Biology*, 146, 903–914.
- Spurr, A.R. (1969) A low-viscosity epoxy resin embedding medium for electron microscopy. *Journal of Ultrastructure Research*, 26, 31–43.
- Taylor, I.S. & Paterson, D.M. (1998) Microspatial variation in carbohydrate concentrations with depth in the upper millimetres of intertidal cohesive sediments. *Estuarine, Coastal and Shelf Science*, 46, 359–370.
- Tolhurst, T.J., Jesus, B., Brotas, V. & Paterson, D.M. (2003) Diatom migration and sediment armouring—an example from the Tagus estuary, Portugal. *Hydrobiologia*, 503, 183–193.
- Underwood, G.J.C., Dumbrell, A.J., McGenity, T.J., McKew, B.A. & Whitby, C. (2022) The microbiome of coastal sediments. In: Stal, L.J. & Cretoiu, M.S. (Eds.) *The marine microbiome*. Switzerland: Springer International Publishing, pp. 479–534.
- Underwood, G.J.C. & Kromkamp, J. (1999) Primary production by phytoplankton and microphytobenthos in estuaries. *Advances in Ecological Research*, 29, 93–153.
- Underwood, G.J.C., Perkins, R.G., Consalvey, M.C., Hanlon, A.R.M., Oxborough, K., Baker, N.R. et al. (2005) Patterns in microphytobenthic primary productivity: species-specific variation in migratory rhythms and photosynthetic efficiency in mixed-species biofilms. *Limnology and Oceanography*, 50, 755–767.
- Vieira, S., Ribeiro, L., Jesus, B., Cartaxana, P. & da Silva, J.M. (2013) Photosynthesis assessment in microphytobenthos using conventional and imaging pulse amplitude modulation fluorometry. *Photochemistry and Photobiology*, 89, 97–102.
- Weilhoefer, C.L., Turner, F. & Matteucci, C.N. (2021) Seasonal relationships between diatom assemblages and environmental conditions vary between Epipelagic- and Epipsammic-dominated tidal flat diatom communities in the Yaquina estuary, Oregon, USA. *Estuaries and Coasts*, 44, 2222–2235.
- Wilhelm, C., Jungandreas, A., Jakob, T. & Goss, R. (2014) Light acclimation in diatoms: from phenomenology to mechanisms. *Marine Genomics*, 16, 5–15.
- Wiltshire, K.H., Blackburn, J. & Paterson, D.M. (1997) The Cryolander: a new method for fine-scale *in situ* sampling of intertidal surface sediments. *Journal of Sedimentary Research*, 67, 977–981.
- Yallop, M., de Winder, B., Paterson, D.M. & Stal, L.J. (1994) Comparative structure, primary production and biogenic stabilization of cohesive and non-cohesive marine sediments inhabited by microphytobenthos. *Estuarine, Coastal and Shelf Science*, 39, 565–582.

SUPPORTING INFORMATION

Additional supporting information can be found online in the Supporting Information section at the end of this article.

How to cite this article: Jesus, B., Jauffrais, T., Trampe, E., Méléder, V., Ribeiro, L., Bernhard, J. M. et al. (2023) Microscale imaging sheds light on species-specific strategies for photo-regulation and photo-acclimation of microphytobenthic diatoms. *Environmental Microbiology*, 25(12), 3087–3103. Available from: <https://doi.org/10.1111/1462-2920.16499>